Scientific Research and Essay Vol.4 (11), pp. 1392-1402, November, 2009
Available online at http://www.academicjournals.org/SRE
ISSN 1992-2248 © 2009 Academic Journals

Full Length Research Paper

Analytical study of effect of disorder on dispersion in steady inertial flows in porous effect

Anil Kumar[1]*, C. L. Varshney[2] and Sajjan Lal[2]

[1]Department of Applied Mathematics, Dronacharya College of Engineering, Greater Noida (U.P.) India.
[2]Department of Mathematics, S.V. College, Aligarh (U.P.) India 202001.

Accepted 25 August, 2009

In this paper, we consider a total dispersion tensor in two-dimensional packed beds consisting of randomly placed parallel cylinders for porosities between 38% to 90%, Peclet numbers up to 100 and Reynolds number up to 20 based on the cylinder diameter and filtration speed. The effective dispersivity is measured by computing the concentration field for a uniform gradient of concentration parallel and normal to the applied pressure gradient. In order to obtain statistically significant ensembles, a sufficiently large number of realizations are generated by repacking the domain and recomputing the dispersivity for porosity, Peclet number and Reynolds number. A comparison is made with transient numerical data in which a fixed concentration is imposed at the boundary. For the Reynolds numbers examined here, inertial effects are depicts to produce a relatively smaller effect, often resulting in a decrease in the dispersivity for a Peclet number. Porosity strongly effects dispersion normal to the bulk flow.

Key words: Dispersion, inertial flows, reynolds number, porous effect, dispersivity.

INTRODUCTION

The transport of a passive scalar (e.g., non-reacting species concentration) through a medium has important applications in many scientific and technological disciplines and has attracted interest in its own right. This dispersive phenomenon was initially modeled by Taylor (1953) for flow through a straight channel and the longitudinal dispersivity was explicitly related to the square of the Peclet number. Carberry and Bretton (1958) depicted axial dispersion of mass in flow through fixed beds. Ebach and White (1958) investigated mixing of fluids flowing through beds of packed solids. Harleman and Rumer (1963) depicted longitudinal and lateral dispersion in an isotropic porous medium. Lee et al. (1996) reported that the predicted transverse dispersivity deviates significantly (as a function of the Peclet number) from the measured values.

Dispersion in disordered porous media haves been examined in numerous experimental studies [Gunn and Pryce (1969) and Han et al. (1985)]. Saffman (1959) investigated a modeled random porous media with randomly oriented capillary tubes and found Fickian dispersion at long times with dispersivity approaching a Peaclet number.

It is apparent that a systematic study of the effects of disorder and Reynolds number on the dispersion in disordered media is missing in the literature. Recent developments in computational fluid dynamics have made it possible o perform direct numerical simulations of the laminar, interstitial velocity and concentration fields. This approach is taken here to investigate the role of disorder and fluid inertia on dispersion in randomly packed beds. Ancona, M.G. (1994) discussed Fully-Lagrangian and lattice-Boltzmann methods for solving systems of conservation equations. For steady-state advection-diffusion problems, however, the time-marching Lattice Boltzmann method is computationally inefficient. Zanchini (2008) investigated mixed convection with variable viscosity in a vertical annulus with uniform wall temperatures. Avedissian and Naylor (2008) studied free convective heat transfer in an enclosure with an internal louvered blind. Chen and Lin (2007) investigated surface waves on viscoelastic magnetic fluid film below down a vertical column. Seddeek and Salem (2007) investigated the effect of an axial magnetic field on the flow and heat transfer about a fluid underlying the axisymmetric spreading surface with temperature dependent viscosity

*Corresponding author. E -mail: dranilkumar06@yahoo.co.in.

and thermal diffusivity. Kumar et al. (2009) studied an analytical study of viscous dissipation effects on MHD natural convection fluid flow along a sphere.

Formulation of the problem

In the present investigation, we are considering the Lattice Boltzmann method for the solution of the Navier-Stokes equations and other transport equations in the Porous effects. The method is developed for problems in which the velocity field is known and the uncoupled transient transport problem is to be investigated.

As in the solution of the Navier-Stokes equations, the advection-diffusion problem is formulated in terms of the particle distribution function $f_i(\mathbf{x},t)$, which is associated with the probability that a particle of solute will lie in the vicinity of $\mathbf{x}$ at time t that is moving with velocity $\mathbf{e}_i$.

$f_i(\mathbf{x},t)\Delta V/C(t)$ = probability of finding a given solute particlein the volume interval ΔV about $\mathbf{x}$ at time t moving with velocity $\mathbf{e}_i$, (1)

Where $C(t)$ is the total concentration of solute in the fluid at time t. For two-dimensions, communication with the four nearest neighbors is required and the microscopic velocity associated with each link is given by;

$$\mathbf{e}_i = \frac{\Delta x}{\Delta t}\left(\cos\frac{\pi(i-1)}{2}, \sin\frac{\pi(i-1)}{2}\right), \quad i = 1,2,3,4 \tag{2}$$

The concentration, ϕ at location $\mathbf{x}$ and time t is found by taking a moment of the particle distribution, in direct analogy with the integral moment from kinetic theory:

$$\sum_i f_i = \phi. \tag{3}$$

The particle distribution satisfies the Boltzmann transport equation in the Porous effects. The discrete velocity analog is given below;

$$\frac{\partial f_i}{\partial t} + \mathbf{e}_i \cdot \nabla f_i = \Omega_i(f(\mathbf{x},t)) + F_i\text{-u/k} \tag{4}$$

Where $\Omega_i\left(f\left(x,t\right)\right)$ is a collision term which accounts for the addition and depletion of particles moving with velocity $\mathbf{e}_i$ due to particle collisions and k is porosity parameter. The term F_i gives rise to a generation term and is defined such that:

$$\sum_i F_i = \Phi \tag{5}$$

where Φ is the imposed mass generation term. The generation process does not directly enter into the flux of solute, the generation term is subject to the constraint, we have:

$$\sum_i F_i \mathbf{e}_i = \mathbf{0}. \tag{6}$$

The discrete velocity Boltzmann, (4), is spatially and temporally discretized using a first-order Lagrangian discretization which yields:

$$f_i(\mathbf{x} + \mathbf{e}_i\Delta t, t + \Delta t) = f_i(\mathbf{x},t) + \Omega_i(f(\mathbf{x},t))\Delta t + F_i\Delta t\text{ -k} \tag{7}$$

Using the linearized, single time relaxation model (Bhatnagar et al., 1954) applied to lattice Boltzmann (Chen et al., 1991), the collision operator is written as:

$$\Omega_i(f) = -\frac{1}{\tau}(f_i - f_i^{(0)}) \tag{8}$$

where $f_i^{(0)}$ is an equilibrium distribution analogous to the Maxwellian distribution. Using this simplification, the Lattice Boltzmann evolution equation is written as:

$$f_i(\mathbf{x} + \mathbf{e}_i\Delta t, t + \Delta t) = f_i(\mathbf{x},t) + \frac{\Delta t}{\tau}\left(f_i^{(0)}(\mathbf{x},t) - f_i(\mathbf{x},t)\right) + F_i\Delta t \text{ +k} \tag{9}$$

It is useful to define a dimensionless relaxation time, $\tau^* = \tau/\Delta t$ and a modified generation term, $F_i' = F_i\Delta t$. Putting in (9) gives the final form of the Lattice Boltzmann evolution equation:

$$f_i(\mathbf{x} + \mathbf{e}_i\Delta t, t + \Delta t) = f_i(\mathbf{x},t) + \frac{1}{\tau^*}\left(f_i^{(0)}(\mathbf{x},t) - f_i(\mathbf{x},t)\right) + F_i' + \text{k} \tag{10}$$

Where the form of the generation term used in this study is given by;

$$F_1' = F_2' = F_3' = F_4' = \frac{\Phi}{4}\Delta t. \tag{11}$$

Since Φ is linear in velocity, the equilibrium distribution takes the form;

$$f_i^{(0)} = A + B\left(\mathbf{e}_i \cdot \mathbf{u}\right), \tag{12}$$

where $\mathbf{u}$ is the known velocity field. The coefficients A and B are found by imposing the following constraints on the process of decay toward equilibrium. The collision process is required to conserve solute are:

$$\sum_i f_i^{(0)} = \phi. \tag{13}$$

And also at equilibrium, the flux of solute is:

$$\sum_i f_i^{(0)} \mathbf{e}_i = \phi\mathbf{u}. \tag{14}$$

Imposing these constraints leads to an equilibrium distribution of the form;

$$f_i^{(0)} = \frac{\phi}{4} + \frac{\phi}{2c^2}\left(\mathbf{e}_i \cdot \mathbf{u}\right) \quad (15)$$

For two-dimensions, where $c = \Delta x/\Delta t$ is the computational speed of sound. The same considerations can be used to find the appropriate distribution for three-dimensional analyses.

Discretization error for advection-diffusion

This section summarizes the derivation of the macroscopic advection-diffusion equation from the microscopic development of the previous section. The starting point is a multi-dimensional Taylor series expansion of the particle distribution about the point $(\mathbf{x},t)$ is given by:

$$f_{\sigma i}\left(\mathbf{x}+\frac{\mathbf{e}_{\sigma i}}{c}\Delta x, t+\Delta t\right) = f_{\sigma i}(\mathbf{x},t) + \sum_{n=1}^{\infty}\frac{1}{n!}\left[(\Delta t)\frac{\partial}{\partial t} + \frac{\Delta x}{c}\mathbf{e}_{\sigma i}\cdot\nabla\right]^n f_{\sigma i}(\mathbf{x},t) + \text{k} \quad (16)$$

This expansion is substituted into the lattice Boltzmann equation, (10) to give,

$$\sum_{n=1}^{\infty}\frac{1}{n!}\left[(\Delta t)\frac{\partial}{\partial t} + \frac{(\Delta x)}{c}\mathbf{e}_{\sigma i}\cdot\nabla\right]^n f_{\sigma i}(\mathbf{x},t) = \frac{1}{\tau^*}\left[f_{\sigma i}^{(0)}(\mathbf{x},t) - f_{\sigma i}(\mathbf{x},t)\right] + F_{\sigma i}' + \text{k} \quad (17)$$

Here the expansion is in terms of a computational Knudsen number, which is defined as the time between collisions relative to the convective time scale of the flow are:

[ ], (18)

Where L/U is the convective time scale, with *L* and *U* as the characteristic length and velocity scales of the flow, respectively. The multi-scale expansions of the particle distribution and evolution time scales are described by:

$$f_{\sigma i} = f_{\sigma i}^{(0)} + \delta_{\Delta t} f_{\sigma i}^{(1)} + \delta_{\Delta t}^2 f_{\sigma i}^{(2)} + \ldots \quad (19)$$

$$\partial_t = \partial_{t_0} + \delta_{\Delta t}\partial_{t_1} + \delta_{\Delta t}^2\partial_{t_2} + \ldots, \quad (20)$$

Where $\partial_t = \partial/\partial t$ is used to indicate the time derivative. Using equation (20) in non-dimensional form, putting these expansions, collecting like powers of the Knudsen number and converting back in dimensional form provides (assuming $1/\tau^* \sim O(1)$):

$$O(\delta_{\Delta t}):\ \left(\partial_{t_o} + \mathbf{e}_i\cdot\nabla\right)f_i^{(0)} = -\frac{U}{L\tau^*}f_i^{(1)} + F_i \quad (21)$$

$$O(\delta_{\Delta t}^2):\ \partial_{t_1}f_i^{(0)} - \frac{L}{U}\left(\tau^* - \frac{1}{2}\right)\left(\partial_{t_o} + \mathbf{e}_i\cdot\nabla\right)^2 f_i^{(0)} + \frac{L}{U}\left(\tau^* - \frac{1}{2}\right)\left(\partial_{t_o} + \mathbf{e}_i\cdot\nabla\right)F_i = -\frac{U}{L\tau^*}f_i^{(2)} + \text{k} \quad (22)$$

From equation (21) has been used to simplify (22). And; (23)

$$O(\delta_{\Delta t}^2):\ \partial_{t_1}\phi - \frac{L}{U\Delta t}\left(\frac{2\tau^* - 1}{4}\frac{\Delta x^2}{\Delta t}\right)\partial_{\alpha\alpha}\phi - \frac{L}{U}\left(\tau^* - \frac{1}{2}\right)\partial_{t_0}\partial_\alpha\left(\phi u_\alpha\right) = 0 \quad (24)$$

The conservation equation is obtained by combining these terms given;

$$\partial_t\phi + \nabla\cdot\left(\mathbf{u}\phi\right) = \mathrm{D}\partial_{\alpha\alpha}\phi + \Phi + E + O\left(\Delta x^2, \Delta t^2\right) \quad (25)$$

where the diffusivity is given by,

$$\mathrm{D} = \frac{2\tau^* - 1}{4}\frac{\Delta x^2}{\Delta t}. \quad (26)$$

And the error E is given by,

$$E = 2\mathrm{D}\Delta t\,\partial_{t_0}\partial_\alpha\left(\phi u_\alpha\right). \quad (27)$$

This error term can be evaluated from several viewpoints. Using (23) it can be written in two other terms are;

$$E = 2\mathrm{D}\Delta t\left(\partial_{t_0}\Phi - \partial_{t_0}^2\phi\right)$$

Or,

$$E = 2\mathrm{D}\Delta t\left\{-\partial_\alpha\left[u_\alpha\partial_\beta\left(\phi u_\beta\right)\right] + \partial_\alpha\left(\Phi u_\alpha\right) + \partial_\alpha\left(\phi\partial_{t_0}u_\alpha\right)\right\} \quad (29)$$

Te expressed as shown in (27), the error term is first order in time, reducing the overall convergence of the method to first order with the time step.

Boundary and initial conditions

The particle distribution is found by determining the high order terms in the expansion expressed in (19). The lowest order term, the equilibrium distribution $f_{\sigma i}^{(0)}$, is given in (15). In order to find higher order terms, the hierarchy of equations given in (6) and (7) are used. In terms of the equilibrium distribution, the first order non-equilibrium term is given by,

$$f_i^{(1)} = \frac{L\tau^*}{U}F_i - \frac{L\tau^*}{U}\left(\partial_{t_o} + \mathbf{e}_i\cdot\nabla\right)f_i^{(0)}. \quad (30)$$

This is expressed in terms of macroscopic quantities by substituting the equilibrium distribution and eliminating the time derivatives using (23) and (24). This yield,

$$f_i^{(1)} = -\frac{\Delta t\tau^*}{\delta_{\Delta t}}\left[-\frac{1}{4}\partial_\beta(\phi u_\beta)+\frac{1}{2}\frac{e_{i\alpha}e_{i\beta}}{c^2}\partial_\alpha(\phi u_\beta)\right]-$$

$$\frac{\Delta x\tau^*}{\delta_{\Delta t}}\left[\frac{1}{4}\frac{e_{i\alpha}}{c}\partial_\alpha\phi\right]+O\left(\frac{\Delta t^2}{\Delta x}\right) \quad (31)$$

$$f_i^{(2)} = -\frac{\Delta t\tau^*\mathrm{D}}{\delta_{\Delta t}^2}\left[\frac{1}{4}\partial_{\alpha\alpha}\varphi-\frac{1}{2}\frac{e_{i\alpha}e_{i\beta}}{c^2}\partial_\alpha\partial_\beta\phi\right]+O\left(\frac{\Delta t^2}{\Delta x},\Delta t^2,\Delta x^2\right) \quad (32)$$

Substituting these expressions for the non-equilibrium contributions in the equation (19) gives the complete particle distribution function in terms of macroscopic quantities are;

$$f_i = \frac{1}{4}\phi+\frac{1}{2}\frac{\Delta t}{\Delta x}\frac{e_{i\alpha}}{c}\phi u_\alpha-\tau^*\Delta x\left[\frac{1}{4}\frac{e_{i\alpha}}{c}\partial_\alpha\phi\right]-$$
$$\tau^*\Delta t\left[\frac{1}{4}\partial_t\phi+\frac{1}{2}\frac{e_{i\alpha}e_{i\beta}}{c^2}\partial_\alpha(\phi u_\beta)-\frac{1}{2}\frac{e_{i\alpha}e_{i\beta}}{c^2}\mathrm{D}\partial_\alpha\partial_\beta\phi\right]+O\left(\frac{\Delta t^2}{\Delta x},\Delta t^2,\Delta x^2\right) \quad (33)$$

where, alternatively, the time derivative term could have been expressed in terms of spatial gradients using the governing equations, we have;

$$\partial_t\phi = -\partial_\alpha(\phi u_\alpha)+\mathrm{D}\partial_{\alpha\alpha}\phi. \quad (34)$$

The four components of the particle distribution are thus given by,

$$f_1 \approx \frac{1}{4}\phi+\frac{1}{2}\frac{\Delta t}{\Delta x}\phi u_x-\tau^*\Delta x\left[\frac{1}{4}\partial_x\phi\right]-\tau^*\Delta t\left[\frac{1}{4}\partial_t\phi+\frac{1}{2}\partial_x(\phi u_x)-\frac{1}{2}\mathrm{D}\partial_{xx}\phi\right] \quad (35a)$$

$$f_2 \approx \frac{1}{4}\phi+\frac{1}{2}\frac{\Delta t}{\Delta x}\phi u_y-\tau^*\Delta x\left[\frac{1}{4}\partial_y\phi\right]-\tau^*\Delta t\left[\frac{1}{4}\partial_t\phi+\frac{1}{2}\partial_y(\phi u_y)-\frac{1}{2}\mathrm{D}\partial_{yy}\phi\right] \quad (35b)$$

$$f_3 \approx \frac{1}{4}\phi-\frac{1}{2}\frac{\Delta t}{\Delta x}\phi u_x+\tau^*\Delta x\left[\frac{1}{4}\partial_x\phi\right]-\tau^*\Delta t\left[\frac{1}{4}\partial_t\phi+\frac{1}{2}\partial_x(\phi u_x)-\frac{1}{2}\mathrm{D}\partial_{xx}\phi\right] \quad (35c)$$

$$f_4 \approx \frac{1}{4}\phi-\frac{1}{2}\frac{\Delta t}{\Delta x}\phi u_y+\tau^*\Delta x\left[\frac{1}{4}\partial_y\phi\right]-\tau^*\Delta t\left[\frac{1}{4}\partial_t\phi+\frac{1}{2}\partial_y(\phi u_y)-\frac{1}{2}\mathrm{D}\partial_{yy}\phi\right] \quad (35d)$$

Where ϕ is the local concentration. Other components which are particularly useful for the prescription of boundary conditions is given by:

$$\sum_i f_i e_{i\alpha} \approx \phi u_\alpha-\frac{\tau^*\Delta x^2}{2\Delta t}\partial_\alpha\phi. \quad (36)$$

Computational determination of effective dispersivity

For solving dispersion in packed beds and other problems in which the macroscopic behavior is of more interest than the microscopic details, it is desirable to formulate an equation which describes the macroscopic phenolmena. This macroscopic convection-diffusion equation can be derived by averaging over many pore sizes are,

$$\frac{\partial\overline{\phi}^f}{\partial t}+\nabla\cdot\left(\overline{\mathbf{u}}^f\overline{\phi}^f\right)=\mathbf{D}:\nabla\nabla\overline{\phi}^f \quad (37)$$

Where $\overline{\psi}^f$ denotes an intrinsic average performed over the fluid phase and defined by,

$$\overline{\psi}^f=\frac{1}{V_f}\int\psi dV_f=\frac{1}{\varepsilon V_T}\int\psi dV_f=\overline{\psi}/\varepsilon, \quad (38)$$

Where ψ is any scalar or vector quantity and V_f is the volume occupied by fluid. However, this equation involves the unknown total dispersion tensor $\mathbf{D}$.

Calculation of effective dispersivity by uniform macroscopic concentration gradient

The steady-state concentration is defined as the flux function of a vector field $\mathbf{B}$ and corresponds to the solution of the advection-diffusion problem when a uniform macroscopic concentration gradient is applied [Bronner, 1980]. The periodic field $\tilde{\mathbf{B}}(\mathbf{x})=\mathbf{B}(\mathbf{x})-\mathbf{x}$ of Brenner (1980) is determined from the steady-state vectorial convection-diffusion equation given by,

(39)

Where $\mathbf{u}'=\mathbf{u}-\overline{\mathbf{u}}^f$ is the difference between the local velocity and the intrinsic average velocity, $\overline{\mathbf{u}}^f$. The concentration gradient is zero at all fluid-solid boundaries which yields the following boundary conditions,

$$\mathbf{n}\cdot\nabla\tilde{\mathbf{B}}=\mathbf{n} \quad (40)$$

Where $\mathbf{n}$ is the outward normal of the particle, directed into the fluid. Periodic boundary conditions are applied at the edges of the computational domain. The local concentration fluctuation, $\phi'=\phi-\overline{\phi}^f$ is calculated from $\mathbf{B}$ for a uniform macroscopic concentration gradient according to,

$$\phi'=-\mathbf{B}\cdot\nabla\overline{\phi}^f. \quad (41)$$

The effective dispersivity is given below;

$$D_{\alpha\beta}=D\left[I_{\alpha\beta}+\frac{1}{V_f}\int_{A_{s-f}}n_\alpha\tilde{B}_\beta dA\right]+\overline{u'_\alpha\tilde{B}_\beta}^f, \quad (42)$$

And

$$D_{\alpha\beta} = D\left[I_{\alpha\beta} + \overline{\partial_\gamma \tilde{B}_\alpha \;\; \partial_\gamma \tilde{B}_\beta}^{\,f} - \overline{\partial_\alpha \tilde{B}_\beta \;\; \partial_\beta \tilde{B}_\alpha}^{\,f} \right]. \quad (43)$$

The steady-state advection diffusion type equation and boundary conditions are given in (39) and (40) is solved using a staggered grid, finite-volume formulation utilizing velocity fields investigated by the lattice Boltzmann method.

Dispersion in a channel

The equations (39) and (40) have an exact solution for the dispersion of a passive scalar in a channel. To calculate the longitudinal dispersivity, the Poiseuille flow solution is substituted into the advection-diffusion equation and (40) is applied in the form of insulating boundary conditions at the upper and lower walls. Putting the resulting expression for $\tilde{\mathbf{B}}$ into either (42) or (43) gives the solution first derived by [Wooding (1960)];

$$D_{xx} = \mathrm{D}\left(1 + \frac{Pe^2}{210}\right), \quad (44)$$

Where the Peclet number here is based on the width of the channel, h and the mean velocity through the channel.

Figure 1 depicts that the relative error in the finite volume results is plotted as a function of grid size. The slope of the relative error with grid size shows that both methods converge with the square of the grid size. However, Figure 1 depicts shows that the discrete version of (42) gives results that are significantly more accurate than those from (43).

Effective conductivity in randomly packed beds

The remainder of the results in this work are found by solving the steady-state advection diffusion equation given in (39) and (40) followed by the calculation of the total effective dispersion tensor according to (42). For no flow conditions, the dispersion problem posed in (37) becomes a conduction problem which can be described by,

$$\frac{\partial \overline{\phi}}{\partial t} = k_e \mathrm{D} \nabla^2 \overline{\phi}^{\,f}, \quad (45)$$

Where the effective conductivity ratio, k_e, is found from the effective dispersion tensor which is isotropic for stationary conditions. The relationship between the effective conductivity ratio and dispersivity obtained by comparing (37) and (45) is;

$$k_e = \varepsilon D_{xx} / \mathrm{D} = \varepsilon D_{yy} / \mathrm{D}. \quad (46)$$

The effective conductivity is compared to results by Cruz and Patera (1995) in Figure 2. Because each realization exhibits slight anisotropy due to random fluctuations, the lateral and transverse dispersivities differ slightly. The averages of these two measures of the dispersivity at zero flow are used to compute the effective conductivity plotted in Figure 2. It is noted that for the cases examined here, the two measures of the dispersivity agree to within 1.5% of the average value. The agreement with the results of Cruz and Patera (1995) is very good despite the fact that the previous results are for a random array of circular cylinders while the current results are for octagonal cylinders.

RESULTS AND DISCUSSION

The comparison is made for one sample of the medium with porosity of 64% at a Peclet number of 5 based on the filtration speed and obstacle size. The concentration profiles obtained from the unsteady simulations are compared to those predicted by the macroscopic equations using the dispersion coefficients found for the same geometry from the steady $\tilde{\mathbf{B}}$ analysis. Along the side of each of these figures is a bar which indicates the intrinsic averaged concentration. This concentration is calculated by averaging along lines normal to the macroscopic concentration gradient. These profiles, as a function of time, are compared to solutions of (37) in Figures. (3) and (4). The agreement between the solution of the macroscopic equations and the transient solute simulations are very good. One discrepancy between the results is the seemingly lower effective diffusivity exhibited by the transient simulations, especially for shorter times. This discrepancy is in complete agreement with findings of Gill and Sankarasubramanian (1970) which depicted that the dispersion coefficient increases with time until reaching its asymptotic result. Computationally this requires an even longer domain and the cost becomes prohibitive. These results depict the asymptotic agreement between measurements of the effective diffusivity coefficients by transient data and long-time $\tilde{\mathbf{B}}$ computations.

Effect of Reynolds number on dispersivity

The remainder of the results in this work are found by solving the steady-state advection diffusion equation given in (39) and (40) followed by the calculation of the total effective dispersion tensor according to (42). The balance between advection and diffusion is governed by the Peclet number and this clearly is the most dominant parameter for characterizing a dispersive process. It is also known that the Reynolds number can independently affect dispersivity by restructuring the flow. Most investigations of dispersivity have not considered inertial effects, solving rather the Stokes equations followed by the convection-diffusion equation. Investigations of inertial flows utilizing regular periodic media have stated that

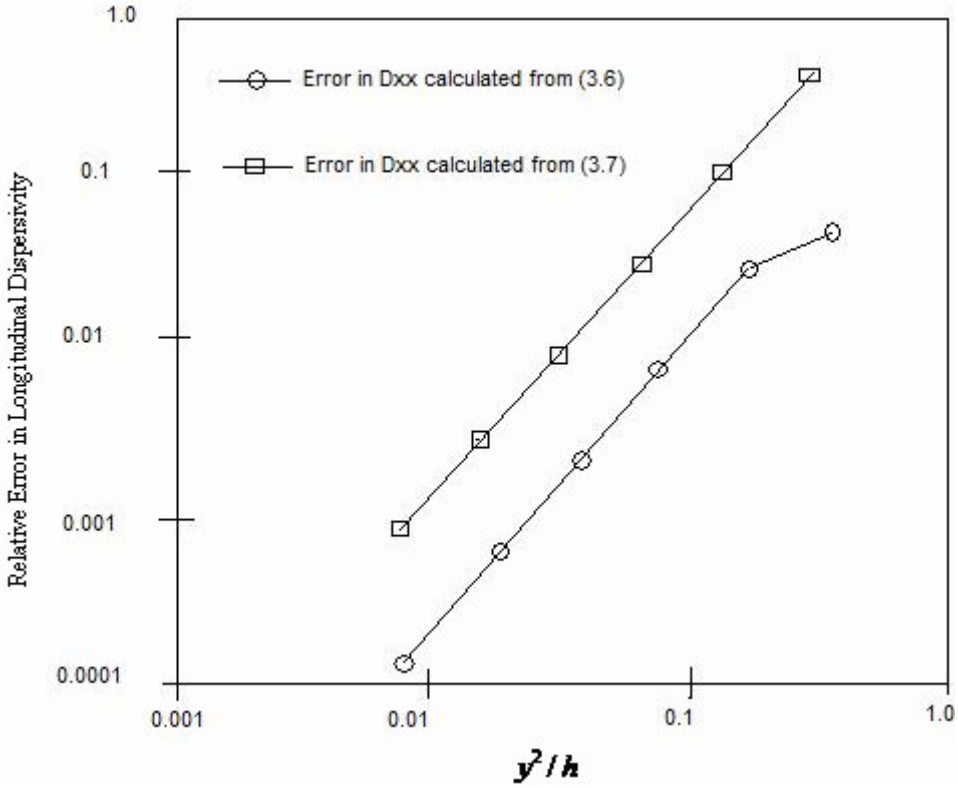

Figure 1. Relative error in calculated values of the longitudinal dispersivity as a function of grid size for Poiseuille flow.

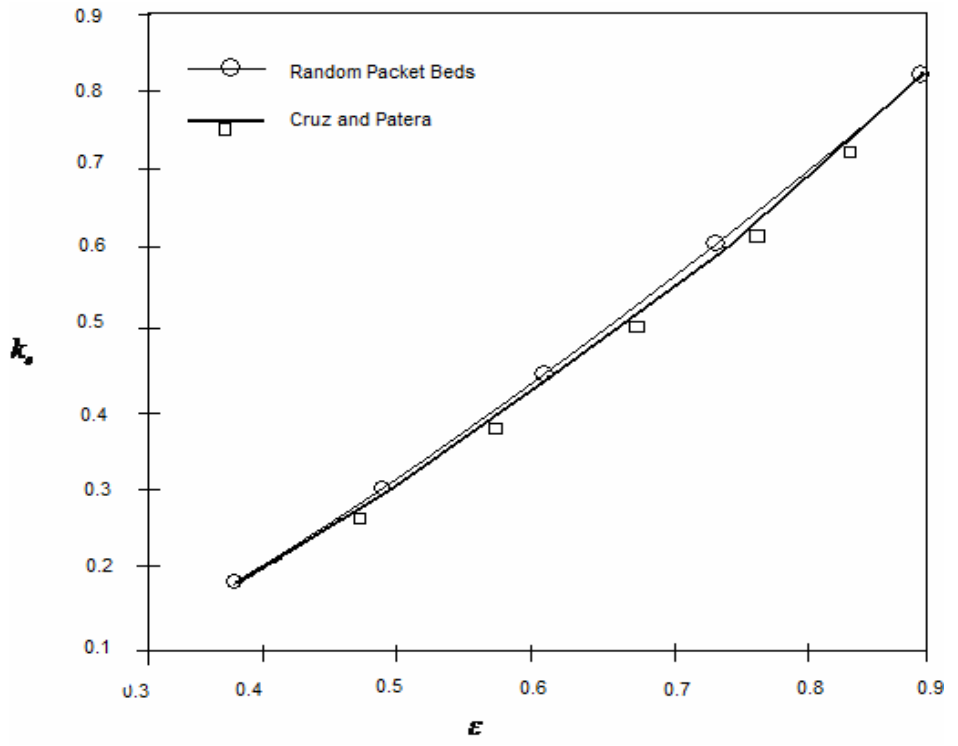

Figure 2. Effective conductivity of two-dimensional packed beds consisting of randomly located parallel octagonal cylinders as a function of porosity.

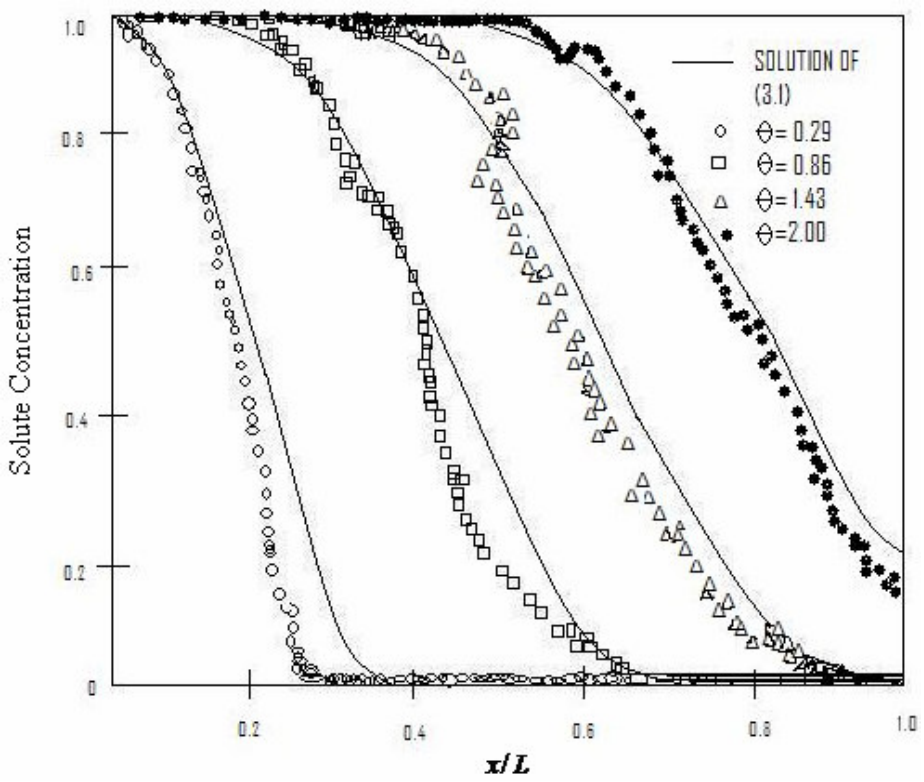

Figure 3. Comparison of longitudinal dispersivity measurements with transient numerical data.

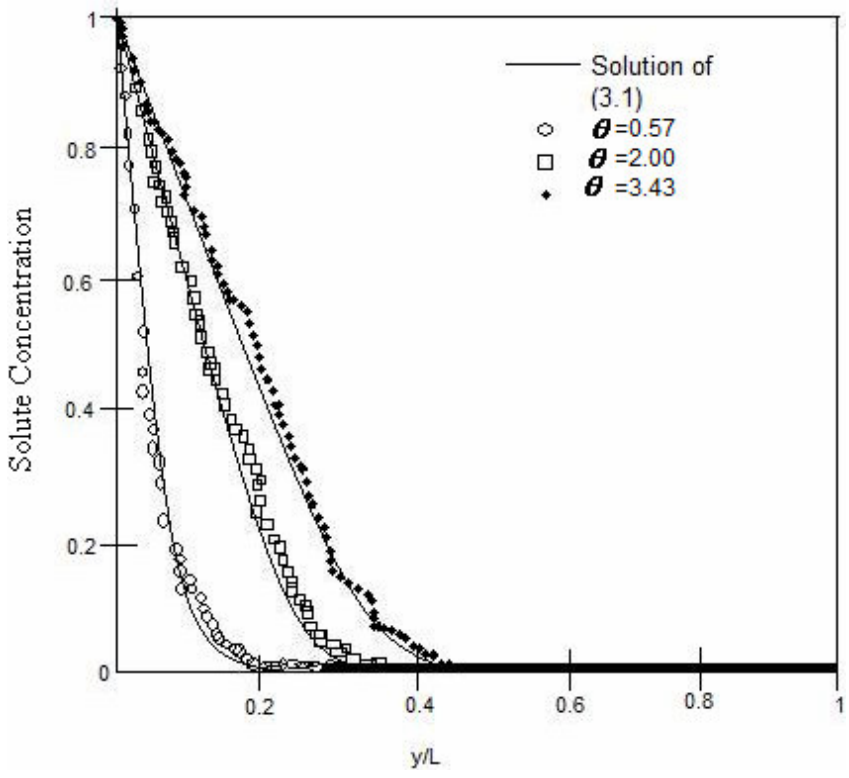

Figure 4. Comparison of transverse dispersivity measurements with transient numerical data.

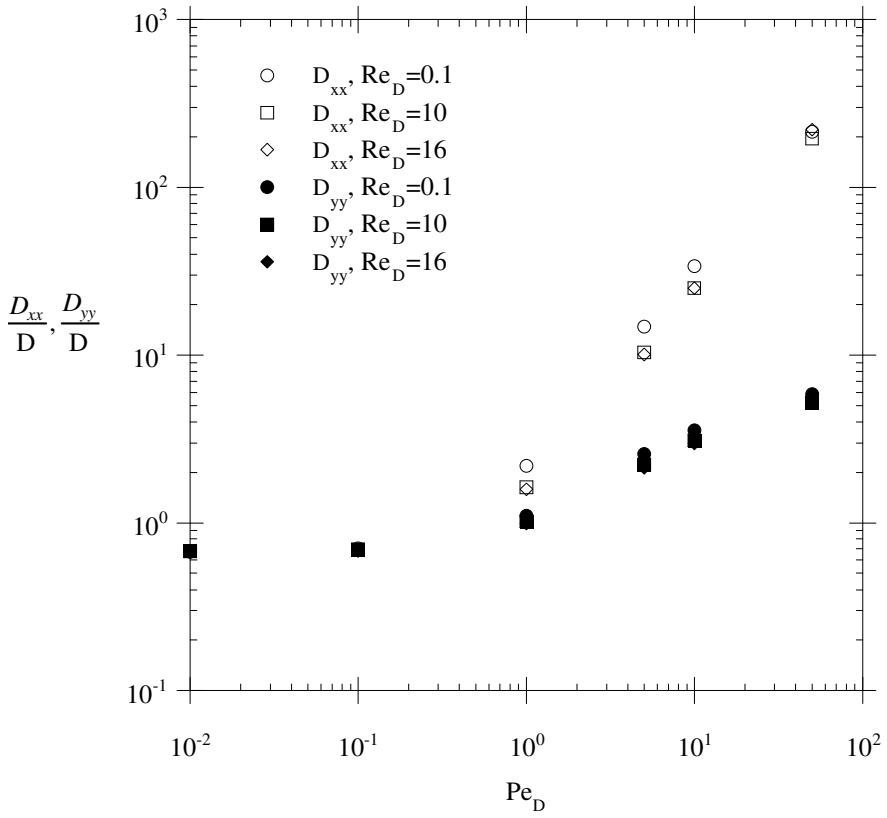

Figure 5. Effect of inertia on longitudinal and transverse dispersivity. The porosity is fixed at 64% and the Reynolds number is varied.

Reynolds number is a minor effect, modifying results by at most 10% (Eidsath, 1981). Figure (5) depicts that the longitudinal and transverse dispersivities as a function of Peclet number, Pe_D, based on the filtration speed and the obstacle size

As for the dependence of dispersivity on Reynolds number for Peclet number, it is shown in Figure 5 the effect is small, at least over the range investigated. Increasing Reynolds number does not necessarily increase dispersion at a Peclet number. In fact, the small effect that Reynolds number does have is generally to decrease dispersivity slightly. Investigations of the velocity distribution in packed beds indicate that as the Reynolds number increases (laminar flow), the velocity field tends to homogenized to some degree. The flow rate in the high speed regions of the flow increase more slowly than those in the low speed regions. This results in a narrower distribution of velocities in the porous medium.

Effect of disorder on dispersivity

Figure 6 compares the Peclet number dependence of dispersivity for ordered and disordered media. The ordered medium has a porosity of 51% and consists of a regular array of inline cylinder which is octagonal in cross-section. All of the data obtained for randomly packed beds is also included. The transverse dispersivity shows a great deal of spread for the various cases. In all cases, however, the transverse dispersivity for dis-ordered media shows a steady increase with Peclet number and greatly exceeds that of the regular medium.

Simulations have shown that the dispersivity increases with the square of the Peclet number over an extended range of Peclet numbers. Figure 6 depicts that, in comparison to regular media, disordered media show an increase in longitudinal dispersivity at lower Peclet numbers. The rate of increase, however, levels off while the growth rate for the regular media increases approaching the quadratic dependence.

Comparison with existing experimental data

Figures (7) and (8), respectively, show the computed longitudinal and transverse dispersivity in packed beds for all Reynolds numbers and porosities along with numerous experimental data and a curve for the periodic array of octagonal cylinders. The porosity of the experimental data is between 0.339 and 0.645. In order to compare to previous results, the data is plotted as a function of the particle Peclet number. For longitudinal dispersivity, shown in Figure (7), the simulation results band around the experimental data with the 38% porosity results

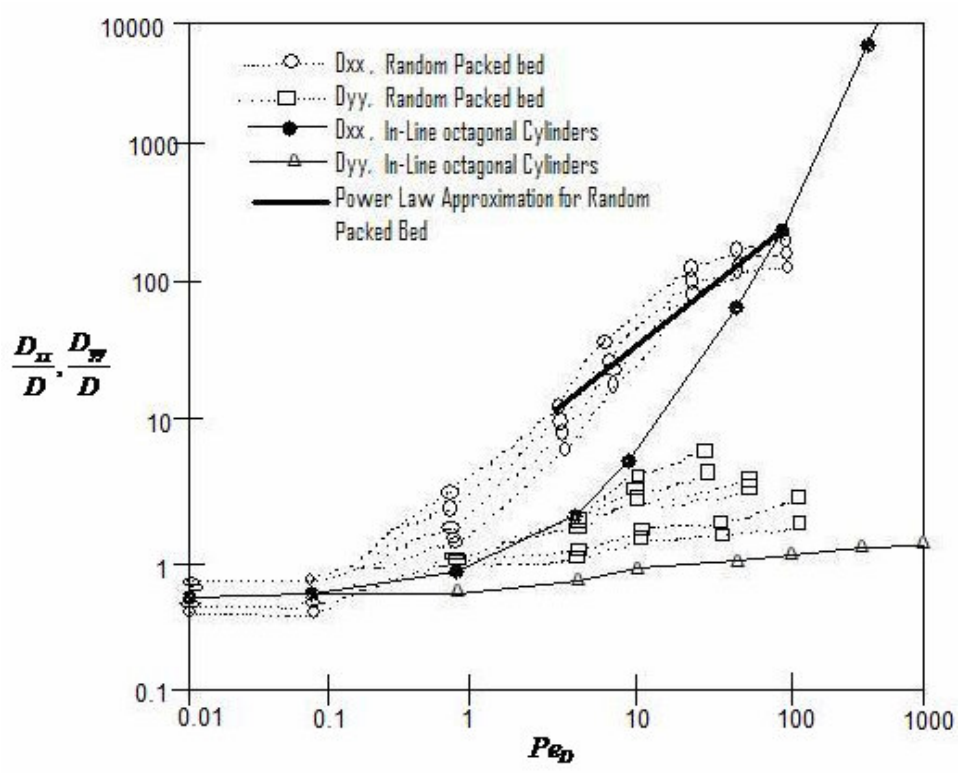

Figure 6. Effect of disorder on longitudinal and transverse dispersivity.

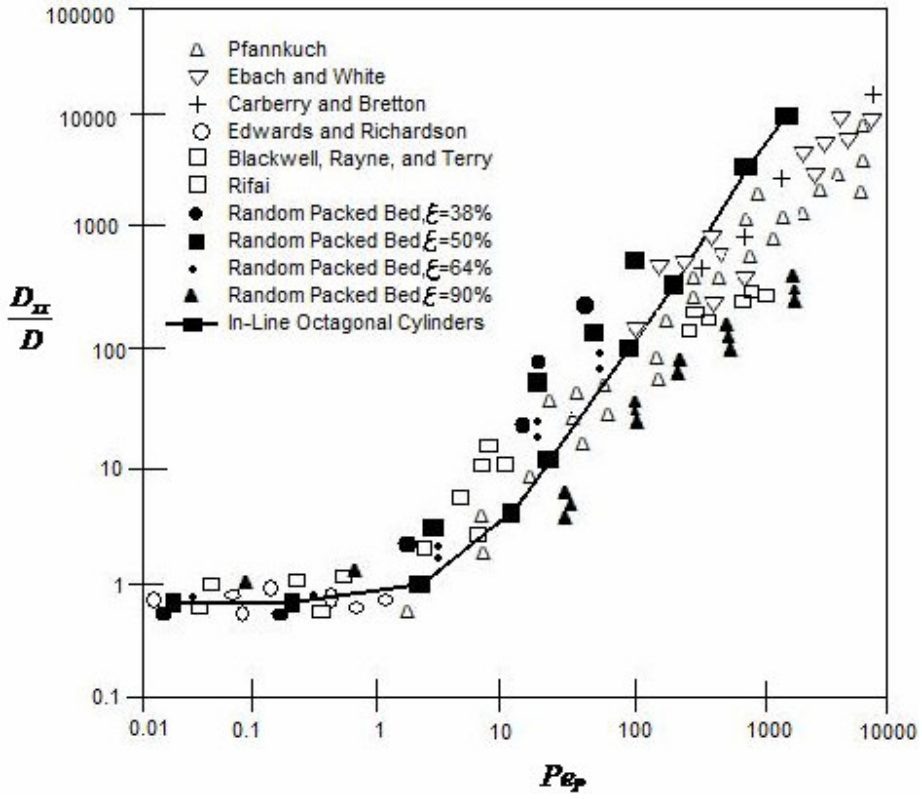

Figure 7. Comparison of present longitudinal dispersivity and experimental data.

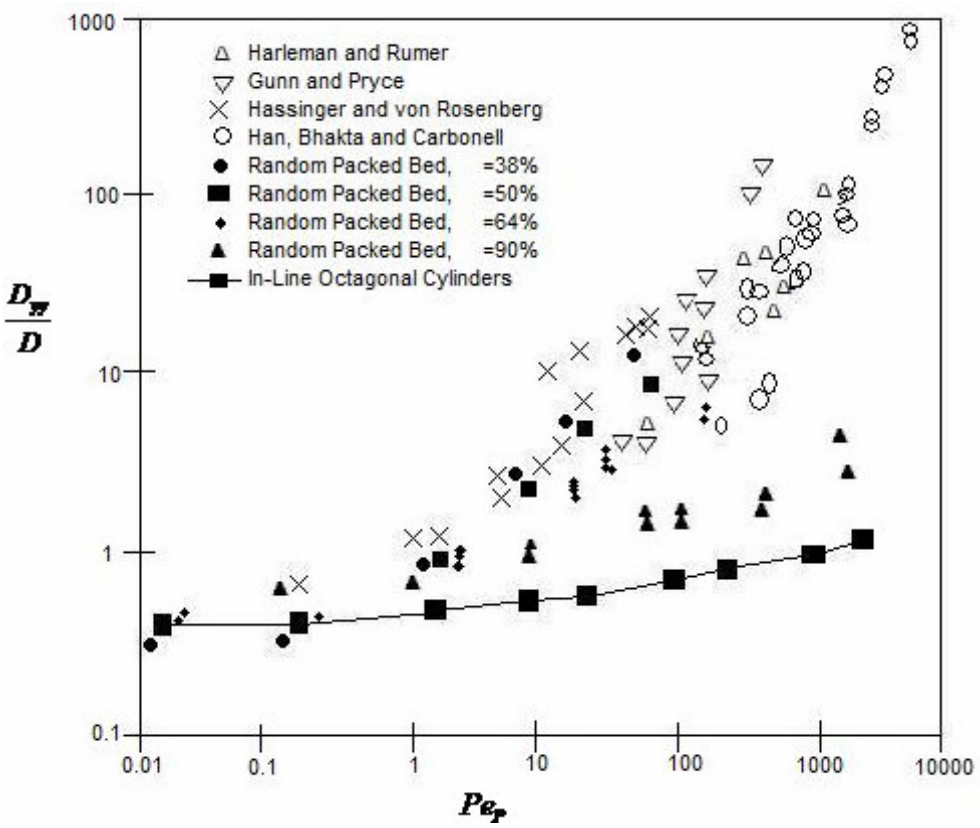

Figure 8. Comparison of present transverse dispersivity and numerical data.

bounding the upper edge of the data and the 90% porosity data bounding the lower edge. The transverse dispersivity comparison in Figure (8) shows equally good agreement at low porosities. Simulations with 38% or 50% porosity compare well with the experimental data, all of which was obtained over the same general range of porosity. At higher porosities, the transverse dispersivity is dramatically under predicted, with the 90% porosity medium approaching the behavior of the periodic array of cylinders.

Conclusions

Simulations of interstitial transport illuminate the role of inertia and disorder on dispersion. For the Reynolds numbers up to Re_D=16 based on the cylinder diameter and filtration velocity, inertial effects are shown to produce a relatively small effect. It is not computationally feasible at this time to perform high Reynolds number simulations in domains which satisfactorily describe packed beds. The authors describe this enhancement to dispersion which arises from growing distance between the solute being advected with the fluid and the slowly diffusing solute contained in hydro dynamical isolated regions. As the size of recirculation zones grow, this effect may lead to an eventual increase in dispersivity with Reynolds number for a Peclet number. Porosity and disorder are seen to play an important role in transverse dispersion normal to the bulk flow. The high speed inclined jets of fluid which are formed in closely packed geometries by the impingement of streamwise jets on constricted regions give rise to much greater transverse dispersion than that observed for higher porosity or ordered media. The histograms of the transverse component of velocity show that the velocity normal to the pressure gradient can exceed the streamwise filtration speed by an order of magnitude for low porosity media (38%) while it rarely exceeds twice the filtration speed for high porosity media (90%). The porosity is
seen to have much less effect on longitudinal dispersion than on transverse dispersion.

REFERENCES

Ancona M (1994). Fully-Lagrangian and lattice-Boltzmann methods for solving systems of conservation equations. J. Comp. Phys. 115: 107.

Avedissian T, Naylor D (2008). Free convective heat transfer in an enclosure with an internal louvered blind. Int. J. Heat and Mass Transfer, 51: 283-293.

Bhatnagar P, Gross EP, Krook MK (1954). A model for collision processes in gases. I. Small amplitude processes in charged and neutral one-component systems. Phys. Rev. 94: 511.

Brenner H (1980). Dispersion resulting from flow through spatially periodic porous media, Philos. Trans. R. Soc. London SER. A297: 81.

Carberry JJ, Bretton RH (1958). Axial dispersion of mass in flow through fixed beds. A.I.Ch.E. J. 4: 367.

Chen PJ, Lin D (2007). Surface waves on viscoelastic magnetic fluid film below down a vertical column. Int. J. Eng. Sci. 45: 905-922.
Chen SY, Chen HD, Martinez D, Matthaeus W (1991). Lattice Boltzmann model for simulation of magnetohydrodynamics. Phys. Rev. Lett. 67: 3776-3779.
Cruz ME, Patera AT (1995). A parallel Monte-Carlo finite-element procedure for the analysis of multicomponent random media. Int. J. Num. Meth. Eng 38: 1087.
Ebach EA, White RR (1958). Mixing of fluids flowing through beds of packed solids. A.I.Ch.E J. 4: 161.
Eidsath AB (1981). Flow and dispersion in spatially periodic porous medium: a finite element study, M.S. Thesis, Department of Chemical Engineering, University of California at Devis.
Gill WN, Sankarasubhramaniam R (1970). Exact analysis of unsteady convection diffusion. Proc. Roy. Soc. A316: 341.
Gunn DJ, Pryce C (1969). Dispersion in packed beds. Trans. Instn. Chem. Engrs. 47: T341.
Han NW, Bhakta J, Carbonell RG (1985). Longitudinal and lateral dispersion in packed beds: Effect of column length and particle size distribution. A. I. Ch. E J. 31: 277.
Harleman DRF, Rumer RR (1963). Longitudinal and lateral dispersion in an isotropic porous medium. J. Fluid Mech. 16: 385.
Kumar A, Varshney CL, Sajjan L (2009). Analytical study of viscous dissipation effects on MHD natural convection fluid flow along a sphere, Presented in National Conference on Recent Drifts, Breaks in Applied Sciences & its Technology for Innovation Management Organized by Deptt. of Applied Sciences and Humanities, KIET, Gaziabad .
Lee CK, Sun CC, Mei CL (1996). Computation of permeability and dispersivities of solute or heat in periodic porous media, Int. J. Heat Mass Transfer, 39: 661.
Saffman PG (1959). A theory of dispersion in porous media. J. Fluid Mech. 6: 321.
Seddeek MA, Salem AM (2007). The effect of an axial magnetic field on the flow and heat transfer about a fluid underlying the axisymmetric spreading surface with temperature dependent viscosity and thermal diffusivity, J. Comp. Mech., 39: 401-408.
Taylor GI (1953). Dispersion of soluble matter in solvent flowing slowly through a tube. Proc. R. Soc. London Ser. A 219: 186-203.
Wooding RA (1960). Instability of a viscous fluid of variable density in a vertical hele-shaw cell. J. Fluid Mech. 7: 501.
Zanchini E (2008). Mixed convection with variable viscosity in a vertical annulus with uniform wall temperatures. Int. J. Heat Mass Transfer, 51: 30-40.